MOLECULAR AND CELLULAR BIOLOGY, July 2004, p. 5767–5775 Vol. 24, No. 13
0270-7306/04/$08.00+0 DOI: 10.1128/MCB.24.13.5767–5775.2004

Abnormal B-Cell Responses to Chemokines, Disturbed Plasma Cell Localization, and Distorted Immune Tissue Architecture in *Rgs1*$^{-/-}$ Mice

Chantal Moratz,[1]† J. Russell Hayman,[3]† Hua Gu,[2] and John H. Kehrl[1]*

Laboratories of Immunoregulation[1] and Immunology,[2] National Institute of Allergy and Infectious Diseases, National Institutes of Health, Bethesda, Maryland 20892, and Department of Microbiology, James H. Quillen College of Medicine, East Tennessee State University, Johnson City, Tennessee 37614[3]

Received 22 December 2003 /Returned for modification 9 January 2004 /Accepted 24 March 2004

Normal lymphoid tissue development and function depend upon chemokine-directed cell migration. Since chemokines signal through heterotrimeric G-protein-coupled receptors, RGS proteins, which act as GTPase-activating proteins for Gα subunits, likely fine tune the cellular responses to chemokines. Here we show that *Rgs1*$^{-/-}$ mice possess B cells that respond excessively and desensitize improperly to the chemokines CXCL12 and CXCL13. Many of the B-cell follicles in the spleens of *Rgs1*$^{-/-}$ mice have germinal centers even in the absence of immune stimulation. Furthermore, immunization of these mice leads to exaggerated germinal center formation; partial disruption of the normal architecture of the spleen and Peyer's patches; and abnormal trafficking of immunoglobulin-secreting cells. These results reveal the importance of a regulatory mechanism that limits and desensitizes chemokine receptor signaling.

The migration of developing lymphocytes into lymphoid tissues, the recirculation of lymphocytes, as well as organization of secondary immune structures such as lymphoid follicles results from a regulated configuration of cell surface adhesion molecules and chemoattractant receptors as well as a spatial overlay of multiple chemoattractant gradients (1, 23, 29, 32). Mechanisms that allow a cell, such as a B-lymphocyte, to interrupt, modify, and prioritize signals from such a milieu of stimuli are essential for efficient and normal immune function. Inappropriate interpretations by cells within such a complex environment is deleterious, leading to inappropriate trafficking, survival, and activation of cells (10, 12, 28, 37). Previous work has detailed B-cell migratory patterns following antigen challenge, including the establishment of germinal centers; cycling within germinal centers; the exiting of memory and antibody-secreting B cells (ASCs) from germinal centers; and the trafficking of ASCs to bone marrow, lamina propria, and other mucosal sites (5, 16, 22, 27, 30, 42, 45). Much of this work has focused on chemokines and their receptors and upon adhesion molecules, while less is known about the signaling mechanisms that allow B cells to efficiently negotiate the complex chemokine gradients likely present in tissues.

Most chemoattracant receptors and all chemokine receptors couple to heterotrimeric G-proteins (1). Activated receptors trigger Gα subunits to exchange GTP for GDP, which dissociates the Gα subunit from βγ heterodimers, leading to the activation of downstream effectors. However, Gα subunits possess an intrinsic GTPase activity that limits the duration of their remaining GTP bound. GTP hydrolysis allows the heterotrimer to reform, and signaling ceases (18, 35). Also limiting the duration of Gα subunits' remaining GTP bound, members of the regulator of G protein signaling (RGS) protein family dramatically increase the intrinsic Gα GTPase activity, a property that defines them as GTPase activating proteins (GAPs). Genetic studies in *Saccharomyces cerevisiae*, *Caenorhabditis elegans*, and *Aspergillus nidulans* first identified such proteins (7, 21, 25). Independently, a mammalian protein termed GAIP was discovered to interact with a Gα subunit (6) and four mammalian proteins designated RGS1, RGS2, RGS3, and RGS4 substituted to various degrees for Sst2p, a yeast protein involved in the desensitization of pheromone signaling (9). Approximately 25 human RGS proteins have now been identified. When tested in standard in vitro GAP assays, most RGS proteins possess GAP activity for the α subunits of the Gi and Gq subfamilies (3, 19, 44).

Since chemokine receptors use Gi and perhaps Gq to transduce intracellular signals, the presence of an RGS protein in target cells could substantially alter the response to chemokine stimulation (20). B-lymphocytes, especially following B-cell activation through their antigen receptors, express RGS1. Consistent with a role for RGS1 in regulating the B-cell responses to chemokines, the expression of RGS1 in B-cell lines dramatically impairs their migratory response to CXCL12 and CXCL13 (4, 33, 38). Because the normal trafficking of B cells depends upon the ligand receptor pairs CXCL12-CXCR4 (34, 46) and CXCL13-CXCR5 (11, 15, 26), a deficiency of *Rgs1* in vivo could alter B-cell development and/or the organization of B cells in lymphoid tissues. To test that possibility we generated *Rgs1*$^{-/-}$ mice.

MATERIALS AND METHODS

Generation of *Rgs1*$^{-/-}$ mice. The targeting construct was designed by replacing the small XbaI fragment located at the end of exon 1 with the neomycin gene. For negative selection of nonhomologous recombination, the thymidine kinase

* Corresponding author. Mailing address: Laboratory of Immunoregulation, National Institute of Allergy and Infectious Diseases, National Institutes of Health, Bldg. 10, Room 11B08, 10 Center Dr., MSC 1876, Bethesda, MD 20892. Phone: (301) 402-4852. Fax: (301) 402-0070. E-mail: jkehrl@niaid.nih.gov.

† C.M. and J.R.H. contributed equally to this work.

gene was placed in opposite transcriptional orientation upstream of exon 1. To generate targeted embryonic stem (ES) cell clones, 30 μg of the linearized targeting vector was electroporated into E14.1 ES cells. ES cells were selected with G418, and resistant clones were screened for homologous recombination. Resultant ES clones were injected into C57BL/6J blastocysts. Chimeric mice were bred, and germ line transmission was documented by Southern blotting. Screening for homozygous *Rgs1*$^{-/-}$ mice was performed by PCR analysis of genomic DNA using *Rgs1*-specific primers. The *Rgs1* mutation was backcrossed five times onto a C57BL/6 background. Mice 6 to 16 weeks old were used for all experiments. Control mice were of the same genetic background as the *Rgs1*$^{-/-}$ mice. Mice were housed under specific-pathogen-free conditions and used in accordance to the guidelines of the Institutional Animal Care Committee at the National Institutes of Health.

RNA isolation and reverse transcription (RT)-PCR analysis. Total RNA was isolated, using a QIAGEN RNA kit with DNase treatment, from cell populations sorted by fluorescence-activated cell sorting or magnetic bead isolation. The cDNA was generated using the Clontech Advantage TM RT-for-PCR kit. For the PCRs, various amounts of cDNA were used with purRE Taq Ready-to-Go PCR Beads (Amersham Biosciences) and 1 μl of each primer. The following primer pairs were used: for β-actin, 5′CCTAAGGCCAACCGTGAAAAG3′ and 5′TCTTCATGGTGCTAGGAGCCA3′; for *Rgs1*, 5′ACGAGCAGCCATC TCCATGCC and 5′CCCAGATTCCAGATGTGGGAT3′; for *Rgs2*, 5′AGCCT GAGTGTTAGGAAAACATGG3′ and 5′TCTTTCATCTCAAACTCTGCTTT C3′; for *Rgs10*, 5′GCAGTCTCGGCTCACTGAAAAGATTC3′ and 5′TATCC AGAGGGAAGGTCTAGCACACTCC3′; for *Rgs13*, 5′ATGAGCAGGCGGA ATTGTTGGA3′ and 5′GAAACTGTTGTTGGACTGCATA3′; and for *Rgs16*, 5′CCATCGGGAAGAGAGGTGGAGTCGC3′ and 5′CCAGGAGTGAGGA AATCAAGACGGG3′. The PCR amplifications were done with the following protocol: 94°C for 3 min initially; followed by 26 to 30 cycles of 30 s at 94°C, 30 s at 58 or 60°C, and 1 min at 72°C; and finally 1 cycle at 72°C for 10 min. The PCR products were separated by electrophoresis in 2% agarose and visualized by staining with ethidium bromide. For each primer pair, the number of PCR cycles chosen was chosen to be in the linear amplification range.

Cell isolation and flow cytometry. Bone marrow cells were isolated from femur bones. A portion was used for RNA preparation and the rest was used to isolate various progenitor B-cell populations using the monoclonal antibodies (MAbs) B220 and CD43 (BD PharMingen) and cell sorting with a FACStar^{Plus} (Becton Dickinson). Thymocytes and T-cell fractions were prepared using the CD4 and CD8 MAbs (BD PharMingen) and cell sorting. B cells from spleen, mesenteric lymph node, peripheral lymph nodes, and Peyer's patches were isolated by negative depletion using biotinylated antibodies to CD4, CD8, GR-1, and CDllc (BD PharMingen) and DynabeadsR M-280 Streptavidin (Dynal Inc., Lake Success, N.Y.). Activated splenic B cells were obtained at various time points following the immunization of mice with a 10% sheep red blood cell (SRBC) solution. In addition, B-cell subsets were isolated from the T-depleted spleen cells by staining remaining cell suspensions with MAbs to CD21, CD23, and B220 (BD PharMingen) and cell sorting. The B-cell populations collected were marginal zone (CD21^{hi} CD23^{low} B220^{+}), follicular cells (CD21^{+} CD23^{+} B220^{+}), and transitional cells (CD21^{dim} CD23^{-} B220^{+}). Plasma cells were isolated by cell sorting T-cell-depleted spleen or Gr-1/Mac-1-depleted bone marrow and staining for B220, immunoglobulin G (IgG), and CD138. The cell populations were greater than 95% pure.

Immunofluorescence microscopy, immunohistochemistry, and immunoblotting. Tissues were embedded in OCT compound, snap frozen, and stored at −80°C. Cryostat sections (10 μm thick) were dried and fixed in acetone or in some cases were formalin fixed and paraffin embedded. In some cases (RGS1 antibody), the acetone-fixed, OCT-embedded sections were rehydrated, treated with 0.15% Triton X-100 in phosphate-buffered saline (PBS) for 5 min, washed with PBS, and quenched with 50 mM NH_4CL in PBS prior to use. For immunofluorescent microscopy the slides were preincubated for 30 min in antibody blocking solution (Dako Corporation) plus 5% serum before incubation with antibodies in a humidified chamber for 1 h at 37°C. Antibodies used were rabbit anti-RGS1 (affinity-purified rabbit antibody raised against an N-terminal RGS1 peptide [33]), anti-IgM (Jackson ImmunoResearch Laboratories), PNA (Vector Laboratories), or anti-B220 or anti-IgG (BD PharMingen). After three washes in PBS a labeled secondary antibody was added for detection, goat anti-rabbit IgG or rabbit anti-goat IgG (Jackson ImmunoResearch Laboratories). The sections were incubated for 1 h at 37°C and then washed with PBS as before and mounted with Fluoromount-G (Southern Biotechnologies). For immunohistochemistry the sections were blocked with a peroxidase blocking reagent and preincubated for 30 min in antibody blocking solution (Dako Corporation) plus 5% serum before incubation with directly biotin-conjugated anti-CD3 and anti-B220 (BD PharMingen) MAbs using the Zymed LAB-SA system (Zymed Laboratories). The sections were visualized using an Olympus BX60 microscope-camera equipped with epifluorescence or in some instances a Leica confocal microscope (NIAID Imaging Unit). The immunoblotting of RGS1 was performed as previously described (33).

Determination of intracellular calcium levels. Splenic cells were isolated, and a single-cell suspension was made. Cells were washed in HBSS buffer (Hanks' balanced salt solution with calcium and magnesium, 10 mM HEPES, and 1% fetal bovine serum), and resuspended at 10^7 cells/ml in HBSS buffer plus the fluorescent calcium probe Indo-1 (indo-1/acetoxymethylester; Sigma or Molecular Probes) at a final concentration of 2 μg/ml. The cells were incubated for 30 min at 30°C while protected from light. Next, the cells were washed with HBSS buffer and resuspended at 10^6 cells/ml in HBSS buffer. Cells were stained with MAbs CD21-FITC, CD23-PE, and B220-APC (BD PharMingen) for 10 min and washed three times in HBSS buffer. The cells were warmed at 37°C for 3 min, loaded into the Time Zero module (Cyteck, Fremont, Calif.) and run at 1,000 cells/s. A baseline was collected for 30 s, and then a sham of 50 μl of HBSS buffer was injected, and finally at 60 s the stimulant was injected. For the desensitization assay cells, a second injection of stimulant was added 2 min after the calcium level returned to baseline. The measurement of calcium flux was performed on a FACSVantage flow cytometer (BD Biosciences) equipped with an argon laser tuned to 488 nm and a Krypton laser tuned to 360 nm. Indo-1 fluorescence was analyzed at 390/20 and 530/20 for bound and free probe, respectively. The data were analyzed using the FlowJo software (Tree Star Inc.). Results are shown as fluorescence ratio (violet/blue).

Chemotaxis assays. Lymphocyte chemotaxis assays were performed using a transwell chamber as previously described (33). Optimal concentrations for CXCL12- and CXCL13-induced chemotaxis were determined in titration experiments. Aliquots of various fractions (input, migrated to chemokine, or migrated in the absence of chemokine) were stained with anti-B220 for 15 min at 4°C, washed, and analyzed on a FACScalibur. Results are shown as the percentage of specific migration, which was calculated by determining the difference between the number of cells in the chemokine-containing well and the number in the well without chemokine, multiplying this difference by 100, and dividing the result by the number of cells put into the assay. For the migration desensitization analyses, cells were exposed either to PBS buffer or to CXCL12 (50 ng/ml; R&D Systems) for 5 min, washed, and then used in a CXCL12 or CXCL13 chemotaxis assay. The results are shown as a ratio of the CXCL12 desensitized to PBS exposed 100 times for either the wild-type or *Rgs1*$^{-/-}$ B cells.

Immunizations, ELISA, and enzyme-linked immunospot (ELISPOT) assay. Serum samples from 6- to 12-week-old animals were assayed for immunoglobulin isotype levels by a sandwich enzyme-linked immunosorbent assay (ELISA) protocol using mouse immunoglobulin standards, goat antibodies specific for mouse immunoglobulin and immunoglobulin isotypes (Southern Biotechnology), and the ABTS developing reagents (Kirkegaard & Perry Laboratories). Optical density was determined with a microplate reader set at 405 nm. Mice were immunized with trinitrophenol-keyhole limpet hemocyanin (TNP-KLH) with adjuvant (100 μg intraperitoneally) and were rechallenged at 14 and 70 days. Serum TNP-specific immunoglobulin levels were analyzed by ELISA. Briefly, 96-well ELISA plates (Nunc) were coated with TNP-OVA (Sigma) overnight at 4°C, washed, and blocked with 5% bovine serum albumin fraction V (Sigma). Serial dilutions of serum were then added to the plates and incubated 4 h at 4°C. After washing horseradish peroxidase-labeled goat anti-mouse immunoglobulin isotype antibodies were added for 2 h at room temperature. The developing reagents were the same as described above. Additional mice were immunized intraperitoneally using either 5 or 50 μg of NP-KLH absorbed to alum. Serum NP-specific immunoglobulin levels were measured as described above except the ELISA plates were coated with NP-bovine serum albumin.

Either OVA-specific IgG or total IgG and IgA antibody secreting cells were identified by conventional ELISPOT analysis. The ELISPOT protocol from BD Biosciences was followed. Briefly, various dilutions of single-cell suspensions prepared from bone marrow, spleen, blood, and lamina propria, from ovalbumin-absorbed to Alum or SRBC-immunized mice, were cultured overnight on nitrocellulose 96-well plates (Millipore) coated either with ova or goat-anti-mouse IgA or IgG (Southern Biotechnologies Inc.). The cells were removed and the captured immunoglobulins were detected with biotinylated goat anti-IgG or anti-IgA (Caltag Laboratories) followed by SA-HRP (BD Biosciences). The plates were developed with an AEC chromogenic substrate solution (BD Biosciences) and spots were enumerated manually using a dissecting microscope.

RESULTS

Cloning the *Rgs1* gene and analysis of *Rgs1* expression. Screening of a mouse spleen cDNA library with a human *RGS1*

cDNA at modest stringency allowed the isolation of an *Rgs1* cDNA. Comparison of the human and mouse predicted amino acid sequences revealed that each encodes a 210-amino-acid protein. The two proteins share identical amino acids at 181 of 210 residues. A previous 5′ RACE analysis of human *RGS1* had extended the original coding sequence 39 nucleotides 5′ to an upstream ATG, thereby adding an additional 13 N-terminal amino acids (MRAAAISTPKLDK; K. Harrison, unpublished observation). *Rgs1* also has an in-frame ATG upstream of the previously published start site that adds a similar number of amino acids (MRAAAISMPRLNK), 10 being identical to those of the human RGS1 N terminus.

A Northern blot analysis of *Rgs1* expression had revealed an increase in B cells following in vivo activation by antigen, while anti-CD40 stimulation had no effect (38). We examined the expression of *Rgs1* in various B- and T-cell subsets isolated from immune tissues by RT-PCR (Fig. 1A). We found a detectable signal in total bone marrow cells and weak signal in $B220^+$ bone marrow cells. Within the B-cell subsets in the spleen *Rgs1* expression predominated in the follicular B cells, with only a low signal detected in marginal zone and transitional B cells. $B220^+$ B cells from mesenteric lymph nodes and purified cells from Peyer's patches also expressed *Rgs1*. Plasma cells isolated by cell sorting for B220 dim/IgG+/$CD138^+$+ cells 1 week following immunization with ovalbumin also expressed *Rgs1*. Among the T-cell subsets from the thymus and spleen, $CD4^+$ cells expressed low amounts of *Rgs1*.

To examine mouse RGS1 protein expression during an immune response we analyzed frozen spleen sections obtained from PBS- and SRBC-immunized mice using an affinity-purified rabbit antibody raised against an N-terminal RGS1 peptide (Fig. 1B). PNA and anti-IgM staining during the time course documented the development of germinal centers in B-cell follicles. In the absence of immunization or in PBS-immunized mice we observed very minimal RGS1 immunoreactivity suggesting that RGS1 expression in the follicular B cells does not exceed the assay detection limit. However, within 3 days of SRBC immunization cells in the B-cell zone reactive with the RGS1 antibody appeared. By 7 days after immunization cells reactive with the anti-RGS1 antibody appeared in the germinal center region. Confirming the specificity of the RGS1 antibody, we did not observe similar reactivity with spleen sections prepared from *Rgs1*-deficient mice (insert in lower right panel of Fig. 1B). Furthermore, a control affinity-purified antibody did not demonstrate significant reactivity with spleen sections from either nonimmunized or immunized mice (data not shown).

Generation of *Rgs1*$^{-/-}$ mice. We screened a murine ES cell genomic library with the *Rgs1* cDNA and isolated a 15-kb NOT1 fragment that encompassed *Rgs1*. Located on mouse chromosome 1, *Rgs1* spans approximately 5 kb and contains five exons, of which the last three contribute to the coding of the RGS domain (Fig. 1C). We produced *Rgs1*$^{-/-}$ mice by inserting a neomycin gene into the first exon of *Rgs1*, which contains the initiating ATG, thereby disrupting the first coding amino acid and the exon splice donor site. Southern blot analysis of wild type and DNA prepared from *Rgs1*$^{-/-}$ mice revealed the appropriate restriction pattern (data not shown). In addition, PCR primers designed to amplify different size products from the wild type and the mutated allele gave bands of

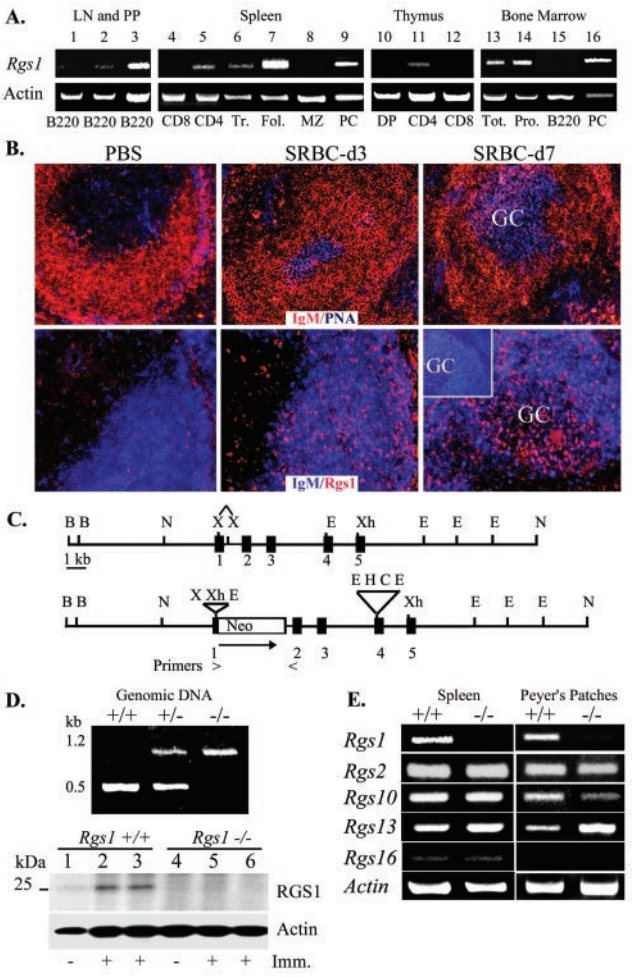

FIG. 1. *Rgs1* expression and generation of *Rgs1*$^{-/-}$ mice. (A) Semiquantitative RT-PCR analysis of *Rgs1* expression in isolated lymphoid subsets as indicated: peripheral lymph node B cells (LN) (lane 1); mesenteric LN B cells (lane 2); Peyer's patch (PP) B cells (lane 3); splenic subsets (CD8 T cells, CD4 T cells, transitional B cells [Tr], follicular B cells [Fol], marginal zone B cells [MZ], and plasma cells [PC]) (lanes 4 to 9); thymus (CD4/CD8 double positive [DP], CD4 single positive [CD4], and CD8 single positive [CD8]) (lanes 10 to 12), and bone marrow (lymphocyte gate [tot], lymphocyte gate $B220^-$ [Pro], $B220^+$, and plasma cells [PC]) (lanes 13 to 16). Data are representative of two to three isolations. Actin levels shown below. (B) Analysis of RGS1 expression in spleens from PBS- or SRBC-immunized mice (day 3 [d3] or d7). Confocal images of splenic sections stained with fluorochrome-labeled anti-IgM (red) versus PNA (blue) or anti-RGS1 (red) versus anti-IgM (blue). Images are representative of sections from two experiments with two to four mice per group. The insert in the lower-right panel shows IgM (blue) versus RGS1 (red) confocal image from an immunized *Rgs1*$^{-/-}$ mouse. (C) Schematic of *Rgs1* targeting to generate *Rgs1*-deficient mice. (D) Verification of *Rgs1* gene targeting. PCR analysis of genomic DNA from wild type, heterozygote, and *Rgs1*-deficient mice. The PCR product from wild-type genomic DNA is 500 bp, while the product generated from *Rgs1*-deficient mice is 1,200 bp. Below is an immunoblot for RGS1 expression using cell lysates (30 μg/lane) from B cells prepared from one wild-type or *Rgs1*$^{-/-}$ mouse and from two wild-type or two *Rgs1*$^{-/-}$ mice immunized with SRBCs 7 days previously. (E) Semiquantitative RT-PCR analysis of various *Rgs* genes in *Rgs1*$^{+/+}$ and *Rgs1*$^{-/-}$ immunized splenic B cells or nonimmunized Peyer's patch B cells. Data are representative of analysis from three pairs of mice.

the predicted size (Fig. 1D, top panel). Mice heterozygous for the *Rgs1* mutation had no apparent abnormalities, and *Rgs1*$^{-/-}$ mice appeared in liters with the expected Mendelian frequencies. Immunoblotting B-cell lysates from wild-type and *Rgs1*$^{-/-}$ mice that had been previously immunized or not for RGS1 expression revealed low levels of RGS1 in unimmunized B cells that increased following immunization and as expected an absence of RGS1 in the *Rgs1*$^{-/-}$ B cells (Fig. 1D, bottom panel). Because *Rgs1* is located in a cluster of *Rgs* genes on chromosome 1 (40) we checked whether the *Rgs1* mutation significantly altered the expression of two genes in the cluster that have lymphoid expression, *Rgs2* and *Rgs13*. In addition, we checked two *Rgs* genes not present in the *Rgs1* cluster, *Rgs10* and *Rgs16*, but which also appear in lymphocytes (2). The *Rgs1*$^{-/-}$ mice lacked *Rgs1* expression in B cells isolated from immunized spleens or in unfractionated cells isolated from their Peyer's patches, while their B cells expressed nearly similar levels of *Rgs2*, *Rgs10*, *Rgs13*, and *Rgs16* as those from control mice (Fig. 1E). The slight increase in *Rgs13* expression may be secondary to increased germinal center formation in the lymphoid tissues of the *Rgs1*$^{-/-}$ mice (see below). Thus, the targeting of *Rgs1* did not appear to significantly alter the expression of clustered or related genes.

The development of lymphoid tissues, including spleen, thymus, mesenteric lymph nodes, and Peyer's patches, in the *Rgs1*$^{-/-}$ mice appeared relatively normal, although occasionally we noted a reduction in the expected sizes of the inguinal and popliteal lymph nodes (data not shown). Flow cytometric analysis of lymph node cells, splenocytes, thymocytes, and bone marrow cells revealed a minimal increase in the number of B220 cell in the bone marrow, a normal distribution of CD4 and CD8 expression on thymocytes, and no significant alteration in the B/T ratio among splenocytes, lymph node cells, or Peyer's patch cells. Of the B-cell subsets in the spleen we noted an increase in the number of cells with a marginal zone phenotype in *Rgs1*$^{-/-}$ B cells compared to control mice (Table 1). However, we did not detect an obvious expansion of the marginal zone on spleen sections.

TABLE 1. Distribution of lymphocytes[a]

Organ or tissue and cell type	% of cell type in mice with indicated genotype (mean ± SE)	
	Rgs1$^{+/+}$	*Rgs1*$^{-/-}$
Spleen		
CD$^+$	19.0 ± 1.3	17.0 ± 1.3
CD8$^+$	12.0 ± 1.3	10.0 ± 1.2
IgM$^+$	62.0 ± 2.6	66.0 ± 1.3
B-cell subsets		
Transitional	14.0 ± 1.3[c]	16.0 ± 4.0[c]
Follicular	75.0 ± 2.4[c]	68.0 ± 8.0[c]
Marginal zone[b,c]	7.0 ± 1.3[b,c]	13.0 ± 3.0[b,c]
Thymus		
CD4$^-$ CD8$^-$	3.8 ± 0.5	3.5 ± 0.8
CD4$^+$ CD8$^+$	84.8 ± 1.9	87.8 ± 0.4
CD4$^+$ CD8$^-$	7.8 ± 0.8	6.1 ± 0.5
CD4$^-$ CD8$^+$	2.8 ± 1.4	2.7 ± 0.5
Bone marrow		
B220^{++}[d] CD43$^-$	12.0 ± 0.6	16.0 ± 1.5
B220^{++}[d] CD43$^-$	14.0 ± 1.7	17.0 ± 0.5
B220$^+$ CD43$^+$	7.0 ± 0.5	9.0 ± 1.7
IgM$^+$ IgD$^+$	8.0 ± 0.2	12.5 ± 3.0
Peripheral lymph nodes		
T	65.0 ± 1.8	69.0 ± 3.0
B	32.6 ± 0.7	24.0 ± 2.1
Mesenteric lymph nodes		
T	61.0 ± 1.3	50.0 ± 3.0
B	35.0 ± 0.7	35.0 ± 2.0
Peyer's patches		
T	14.0 ± 3.6	13.0 ± 2.1
B	81.0 ± 4.6	84.0 ± 11.0

[a] Values presented are based on results for four mice 6 to 8 weeks old.
[b] Significant difference, $P = 0.002$ (Student's t test).
[c] Percentage of B-cell population.
[d] Signs indicate levels of B220 expression.

B cells from *Rgs1*$^{-/-}$ mice exhibit abnormal responses to chemokine stimulation. Since chemokines often elicit an increase in intracellular calcium, we measured the level of intracellular Ca^{2+} of either wild-type or *Rgs1*$^{-/-}$ B cells following their exposure to CXCL12. Since *Rgs1* expression predominated in follicular B cells, we examined the response of these cells. The exposure of *Rgs1*$^{-/-}$ follicular B cells to CXCL12 resulted in an increased and prolonged elevation of intracellular Ca^{+2} levels compared to that of wild-type follicular B cells (Fig. 2A). The 75th percentile of fluorescence for the Ca^{2+} parameter is shown as a function of time (the line is smoothed using a Gaussian smoothing algorithm). Next, we examined whether the absence of *Rgs1* affected chemokine receptor desensitization by measuring the intracellular Ca^{2+} flux following a repeat chemokine exposure. Reexposure of wild-type follicular B cells to CXCL12 led to a reduced Ca^{+2} influx compared to the original. Conversely, reexposure of the *Rgs1*$^{-/-}$ follicular B cells to CXCL12 augmented their intracellular Ca^{2+} response compared to the original exposure (Fig. 2A). Again, the 75th percentile of fluorescence for the Ca^{2+} parameter is shown as a function of time. We found similar results when we substituted CXCL13 for CXCL12 (data not shown).

The loss of *Rgs1* affected B-cell migration as documented by transwell chemotaxis assays. The lack of *Rgs1* led to a greater number of B220$^+$ B cells moving in response to CXCL12 at each concentration tested (Fig. 2B). This was slightly exaggerated when we examined the responses of B cells from immunized mice (Fig. 2C). Few *Rgs1*$^{+/+}$ germinal center B cells migrated to either CXCL12 or CXCL13 (1.5% of the PNA$^+$ B220$^+$ cells); however, a small but significant percentage of the *Rgs1*$^{-/-}$ germinal center B cells (6% of the PNA$^+$ B220$^+$ cells) did so. While the percentage of B cells from the *Rgs1*$^{-/-}$ mice that moved in the transwell chamber assays significantly exceeded those from wild-type mice, the dose-response curve, percentage of cells migrating versus concentration of chemokine, was minimally affected by the loss of *Rgs1* expression. Similar to wild-type B cells, pertussis toxin treatment, which inhibits Gi activation, completely blocked the migration of *Rgs1*$^{-/-}$ B cells. In contrast to the B-cell findings, the *Rgs1*$^{-/-}$ T cells migrated normally in response to CXCL12, CCL3, CCL4, CCL19, CCL21, or CCL22 (data not shown).

Next, we checked the effect of *Rgs1* deficiency on the migra-

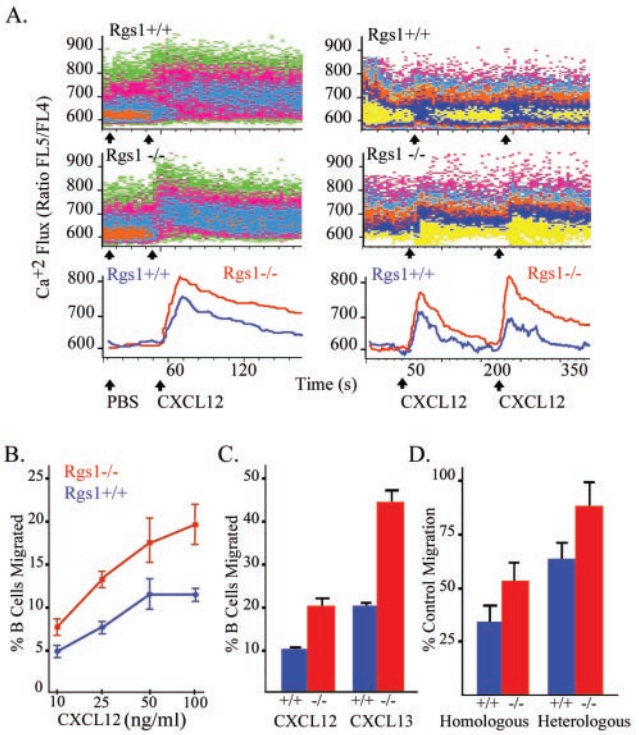

FIG. 2. Alterations in chemokine receptor signaling in *Rgs1*$^{-/-}$ B cells. (A) Intracellular calcium response to CXCL12. Indo-1 loaded splenic cells from *Rgs1*$^{+/+}$ and *Rgs1*$^{-/-}$ mice were stimulated with CXCL12 (left panels). Responses of the follicular B cells are shown. The data are shown as density plots and overlay histograms. The overlay histogram shown below is the 75th percentile of fluorescence for the Ca^{2+} parameter as a function of time (the line is smoothed using a Gaussian smoothing algorithm). The increases in intracellular Ca^{2+} of wild-type and *Rgs1*-deficient splenic B cells following a primary and a secondary exposure to CXCL12 are also shown (right panels). Cells were stimulated with CXCL12 (50 ng/ml), and the Ca^{2+} levels were allowed to return to baseline, after which the cells were rechallenged with CXCL12. Gated $B220^+$ follicular B-cell responses were measured and plotted as above. (B) Migration of splenic $B220^+$ cells to CXCL12. Triplicate transwell assays were done to measure migratory responses to increasing concentrations of CXCL12 of $B220^+$ spleen cells prepared from wild-type and *Rgs1*$^{-/-}$ mice. A significant difference existed between *Rgs1*$^{-/-}$ and *Rgs1*$^{+/+}$ B cells at each concentration (Student's *t* test: 10 ng, $P = 0.01$; 25 ng, $P = 0.002$; 50 ng, $P = 0.004$; 100 ng, $P = 0.001$). Results are representative of one of five experiments performed. (C) Migration of splenic $B220^+$ cells from immunized mice. Splenic cells from *Rgs1*$^{+/+}$ and *Rgs1*$^{-/-}$ mice 7 days post-SRBC immunization were used in a transwell chemotaxis assay to determine the migration of $B220^+$ cells to optimal concentrations of CXCL12 or CXCL13. The percentage of B cells migrating in response to each chemokine is shown. Student's *t* test was used to compare the significance of wild-type and *Rgs1*$^{-/-}$ results in response to CXCL12 ($P = 0.02$) and CXCL13 ($P = 0.01$). (D) Desensitization of chemokine-induced migration. Splenic B cells were prestimulated with CXCL12 (50 ng/ml), the chemokine was removed, and the cells were reexposed to the same concentration of CXCL12 (homologous) or CXCL13 1,000 (ng/ml) (heterologous). The data are shown as percentages of primary migration (right panel, primary migration is the percentage of wild-type or *Rgs1*$^{-/-}$ splenic B cells that migrate in response to either CXCL12 or CXCL13). Significant differences between wild-type and *Rgs1*$^{-/-}$ B cells were found (Student's *t* test: homologous, $P = 0.02$; heterologous, $P = 0.006$).

tory response to a secondary chemokine challenge. We exposed B cells to CXCL12, washed the cells, and measured subsequent migratory responses to CXCL12 or CXCL13. The wild-type cells exhibited both a homologous, reduced response to a rechallenge with CXCL12 and heterologous desensitization, a reduced response to rechallenge with CXCL13. The *Rgs1*$^{-/-}$ B cells exhibited a decreased ability to desensitize following a rechallenge with CXCL12 or CXCL13 (Fig. 2D).

The spleen and Peyer's patches in *Rgs1*$^{-/-}$ mice. Because the spleen sections prepared from *Rgs1*$^{-/-}$ mice, but not from wild-type mice, had a significant number of germinal centers even the absence of immunization, we examined the kinetics of germinal center development in these mice following immunization with SRBC. We estimated the number of germinal centers by determining the density of PNA^+ $B220^+$ clusters in timed tissue sections (clusters were defined as containing greater than 25 PNA^+ $B220^+$ cells). Germinal centers appeared more rapidly, reached a higher density, and resolved more slowly in the spleens from the *Rgs1*$^{-/-}$ mice compared to controls (Fig. 3A and B). At day 30 postimmunization, wild-type spleens had resolved their germinal center reaction while *Rgs1*$^{-/-}$ spleens still had approximately half their peak number. Following immunization the *Rgs1*$^{-/-}$ spleens lost the normal sharp delineation between their B and T zones and had oddly shaped periarterial lymphatic sheaths (Fig. 3C).

Prior to immunization Peyer's patches from *Rgs1*$^{+/+}$ and *Rgs1*$^{-/-}$ mice appeared normal; however, while the wild-type Peyer's patches increased in size upon immunization, Peyer's patches from the *Rgs1*$^{-/-}$ mice shrank dramatically (Fig. 4A). The reduction was apparent upon histological examination, and staining for IgM expression revealed an apparent large efflux of cytoplasmic IgM-positive cells from the Peyer's patches of the *Rgs1*$^{-/-}$ mice (Fig. 4B). In contrast, the histological appearance of the peripheral lymph nodes from the *Rgs1*$^{-/-}$ mice appeared much more normal following immunization.

Localization of immunoglobulin-secreting cells. Because of the abnormalities in Peyer's patches following immunization and because we noted a reduction in the number of cytoplasmic IgG-positive cells in the bridging channels of splenic red pulp from *Rgs1*$^{-/-}$ mice (Fig. 5A), we performed ELISPOT assays to assess the number of ASCs present in the spleen, blood, bone marrow, and lamina propria following immunization with ovalbumin or SRBC. At days 7 and 14 in the *Rgs1*$^{-/-}$ mice we found a reduction in the ovalbumin-specific IgG ASCs in the spleen and bone marrow but an increase in the level of these ASCs in blood compared to that observed in wild-type mice. At day 30 in the *Rgs1*$^{-/-}$ mice the numbers of ovalbumin-specific IgG ASCs remained elevated in the blood and decreased in the bone marrow, but in contrast to the earlier time points they were elevated in the spleen compared to that observed in wild-type mice (Fig. 5B). A similar pattern emerged when we examined IgG, IgA, and IgM ASCs following immunization with SRBCs. At both day 7 and day 14 we found decreased numbers of ASCs in the spleen and in the bone marrow, with increased numbers in the blood (data not shown). In addition, we found a marked reduction in the number of IgA ASCs in the lamina propria of the *Rgs1*$^{-/-}$ mice versus those in wild-type mice (Fig. 5B). The low numbers of IgG, IgA, and IgM ASCs detected prior to immunization did

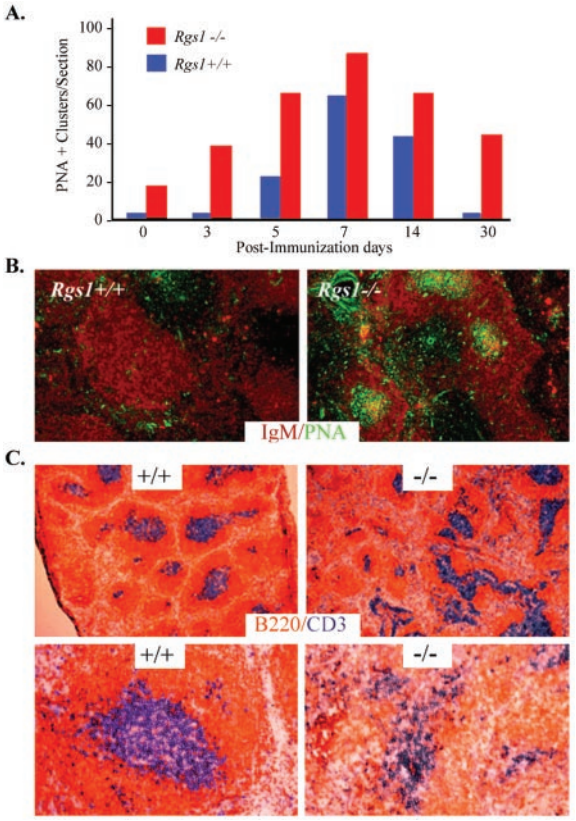

FIG. 3. Germinal center formation in *Rgs1*$^{-/-}$ mice. (A) Time course analysis of an SRBC-induced germinal center response in *Rgs1*$^{+/+}$ and *Rgs1*$^{-/-}$ mice. Splenic sections from the indicated day post-SRBC immunization were stained with anti-IgM and PNA to identify germinal center clusters. PNA^{+} clusters in B-cell follicles from similarly sized longitudinal cross-sections of immunized spleens were counted, and the averages of three sections per animal were graphed. Three animals per time point are shown. The PBS-injected mice are shown at day 0. Significant differences between wild-type and *Rgs1*$^{-/-}$ mice were found at days 1, 3, 5, and 30 (Student's *t* test: day 0, $P = 0.05$; day 3, $P = 0.003$; day 5, $P = 0.02$; day 7, $P = 0.2$; day 14, $P = 0.1$; day 30, $P = 0.0001$). (B) Splenic sections from wild-type and *Rgs1*$^{-/-}$ mice 30 days post-SRBC immunizations stained with anti-IgM (reddish brown) and PNA (green) are compared. (C) Architecture of B- and T-cell zones in the spleen. Splenic sections 30 days postinjection with TNP-KLH plus adjuvant from *Rgs1*$^{+/+}$ or *Rgs1*$^{-/-}$ mice were stained with CD3 (blue) and B220 (orange). The sections are shown at a magnification of ×60 and are representative of the four to six animals per group used in the experiment.

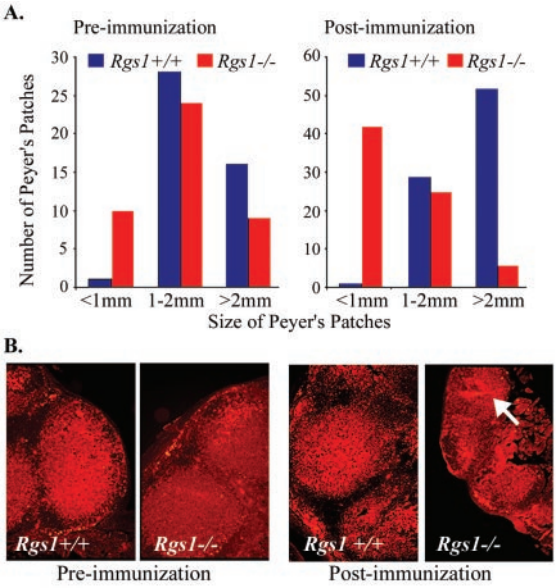

FIG. 4. Alterations in Peyer's patches following immunization of *Rgs1*$^{-/-}$ mice. (A) Effect of immunization on the size of Peyer's patches. Peyer's patches from wild-type and *Rgs1*$^{-/-}$ mice were isolated and measured before and 7 days after SRBC immunization. The numbers of Peyer's patches with diameters of <1, 1 to 2, or >2 mm from wild-type and *Rgs1*$^{-/-}$ mice prior to and after immunization were determined (five animals per group). Unimmunized mice had six to nine Peyer's patches. (B) Photomicrographs of *Rgs1*$^{+/+}$ or *Rgs1*$^{-/-}$ Peyer's patches. Shown are wild-type and *Rgs1*$^{-/-}$ Peyer's patches immunostained for IgM expression (magnification, ×100) obtained either prior to or after SRBC immunization.

not differ significantly between wild-type and *Rgs1*$^{-/-}$ mice (data not shown).

Antibody levels and response to immunization. Despite the alterations in plasma cell trafficking and distortion of the immune architecture in the *Rgs1*$^{-/-}$ mice, we detected only minor abnormalities in the levels of immunoglobulins in serum and in the antibody responses to strong immunogens. The *Rgs1*$^{-/-}$ mice had levels of IgA, IgM, and IgG subtypes in serum similar to those observed in control mice, with the exception of a 10-fold and a 3-fold increase in IgG2a and IgG2b, respectively (data not shown). Serum antibody responses following immunization of the mice with TNP-KLH uncovered a delay in the IgG1 and IgG3 anti-TNP responses; however, eventually the *Rgs1*$^{-/-}$ mice achieved titers similar to those observed with wild-type mice (Fig. 6A). The kinetics of the IgM antibody response appeared similar in both sets of mice. Surprisingly, despite the previously noted shrinkage of Peyer's patches following immunization of *Rgs1*$^{-/-}$mice, the specific IgA response detected in the sera of the *Rgs1*$^{-/-}$ mice exceeded those of the wild-type mice at every time point tested (Fig. 6A). Reimmunization with TNP-KLH revealed an intact memory response in the *Rgs1*$^{-/-}$ mice (Fig. 6B). Finally, we tested whether the disruption of *Rgs1* altered the affinity maturation of an anti-NP response. An ELISA performed with day 10 and day 21 serum samples collected from wild-type and *Rgs1*$^{-/-}$ mice previously immunized with NP-KLH revealed comparable ratios of high-affinity IgG1 anti-NP antibody to the total IgG1 anti-NP antibody (Fig. 6C).

DISCUSSION

To properly position themselves in and to move out of lymphoid compartments, cells need to integrate temporal and spatial information delivered by a set of chemokine gradients, likely navigating in a stepwise fashion from one gradient to another (13). To do so, cells must eventually turn away from a primary chemokine source, migrating down the primary chemokine gradient and up a gradient towards a new chemokine source. Desensitization of signaling through the primary chemokine receptor may allow the cells to switch their allegiance to a second chemokine source. Here we show that RGS1 participates in a desensitization mechanism operant in B-lympho-

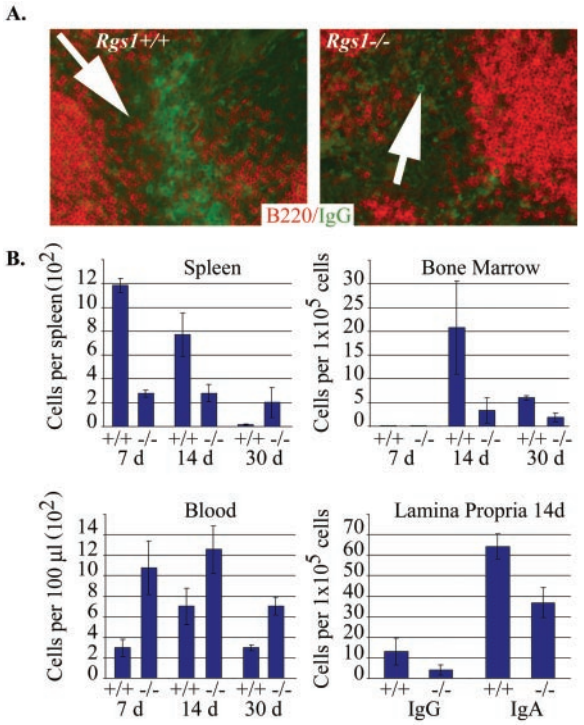

FIG. 5. Analysis of the generation and localization of ASCs following immunization. (A) IgG-positive cells located in the spleen of *Rgs1*$^{+/+}$ or *Rgs1*$^{-/-}$ mice at 14 days following immunization. Arrowheads identify bridging channels. The sections labeled for IgG (green) expression were also stained with B220 (orange) (magnification, ×200). (B) ELISPOT analysis of *Rgs1*$^{+/+}$ or *Rgs1*$^{-/-}$ mice following OVA or SRBC immunization. Splenic, bone marrow, and peripheral blood cells were collected and used to enumerate the number of OVA-specific IgG ASCs. Total IgG and IgA ASCs were enumerated from lamina propria lymphocytes following SRBC immunization. The results from the wild-type and *Rgs1*$^{-/-}$ mice were statistically different at each time point examined for the cells isolated from spleen, bone marrow, blood, and lamina propria ($P < 0.03$ by Student's *t* test).

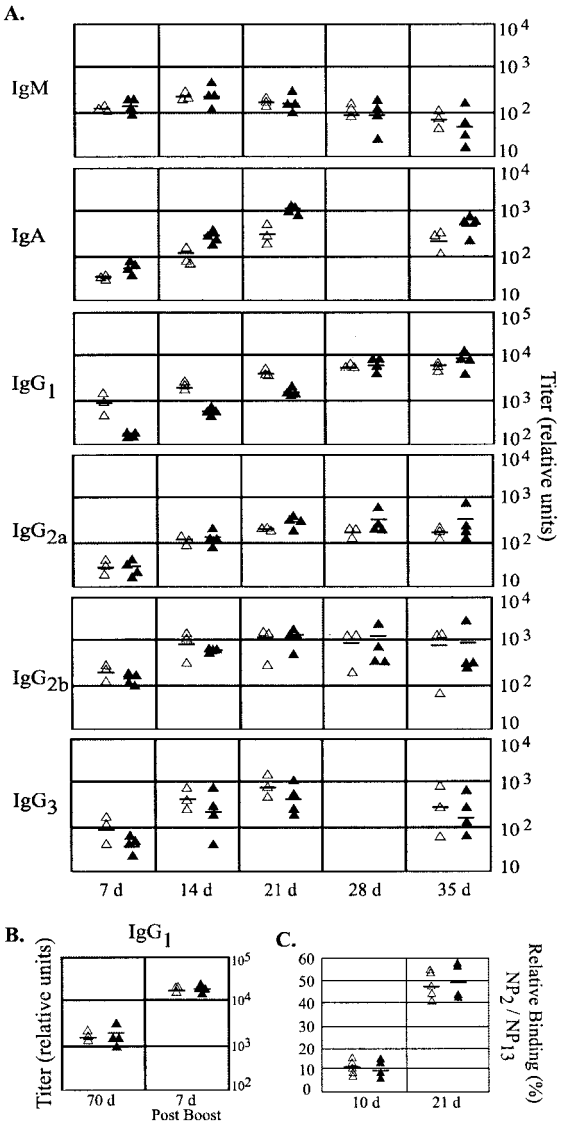

FIG. 6. Humoral immune responses in wild-type and *Rgs1*$^{-/-}$ mice. (A) Specific antibody response to TNP-KLH. Relative titer of indicated immunoglobulin isotypes from wild-type and *Rgs1*$^{-/-}$ mice 7, 14, 21, 28, and 35 days following immunization. The day 28 IgA and IgG3 values were not determined. Results from individual mice are shown. (B) B-cell memory. Wild-type and *Rgs1*$^{-/-}$ mice were boosted with TNP-KLH and serum collected 1 week later. Relative titers from individual mice are shown (left panel). (C) Affinity maturation of the IgG response. Serum from wild-type and *Rgs1*$^{-/-}$ mice 10 and 21 days post-TNP-KLH immunization were assessed for the binding to NP_2 and NP_{13}. Results from individual mice are shown as relative binding percentage.

cytes. *Rgs1*$^{-/-}$ B cells fail to undergo proper desensitization and are supersensitive to certain chemokines. The lack of this desensitization mechanism may help explain some of the phenotypes observed in these mice.

Besides RGS proteins, mammalian cells use other mechanisms to desensitize signaling through G-protein-coupled receptors, including receptor uncoupling, G-protein degradation, and receptor sequestration. However, the failure of the *Rgs1*$^{-/-}$ B-cell CXCR4 and CXCR5 receptors to undergo rapid homologous desensitization unveiled the importance of the RGS mechanism in these cells. Previous results obtained by expressing mutant Gα subunits insensitive to RGS proteins in pertussis-toxin-treated cells (36), blocking endogenous RGS proteins with specific antibodies (8), reducing endogenous *RGS* mRNAs with ribozyme technology (43), and analyzing opioid antinociception in *Rgs9*$^{-/-}$ mice (14) have implicated RGS proteins in the desensitization of other G-protein linked signaling pathways. While additional studies examining other RGS proteins and different G-protein-coupled receptor-linked signaling pathways will be required to understand the relative importance of the various desensitization mechanisms, the data reported here suggest that RGS proteins have a prominent role in the desensitization of chemokine receptor signaling. Furthermore, the involvement of *Rgs1* in the rapid desensitization that occurs following chemokine exposure of wild-type B cells suggests that the initial G-protein signaling shifts RGS1 from an inactive to an active state. This may involve the translocation of RGS1 from a cytosolic pool to the cell membrane as G-protein signaling causes several other RGS proteins to similarly translocate via a process that depends upon

their N termini (9, 41). Alternatively, RGS proteins may be recruited into lipid rafts where chemokine receptors and Gα subunits likely reside (31).

Besides their role in desensitization, the level of an RGS protein within a cell can set a response threshold. Consistently, a higher percentage of the *Rgs1*$^{-/-}$ B cells migrated to CXC12 than did the control cells, suggesting that unstimulated normal splenic B cells express sufficient amounts of RGS1 to alter the threshold at which a response occurs. The in situ demonstration of the presence of RGS proteins has proven difficult, perhaps because high levels of these proteins in cells grossly impairs signaling through multiple G-protein-linked signaling pathways, a situation most cells generally avoid. Yet RGS1 levels can be substantially raised in B cells, and the most pronounced disarrangements in lymphoid architecture occurred following immunization, which normally elevates B-cell *Rgs1* expression levels. The levels of RGS1 in B cells may act as an intracellular rheostat controlling both the magnitude of a G-protein-coupled receptor-triggered response as well as the response threshold.

How do the signaling data explain the phenotypes observed in the *Rgs1*$^{-/-}$ mice, in particular: (i) the early and excessive germinal center formation following immunization; (ii) the abnormal splenic architecture, which is accentuated following immunization; and (iii) the shrinkage of Peyer's patches and improper trafficking of ASCs. The first phenotypic abnormality suggests an enhanced recruitment of B cells into the nascent germinal centers in the *Rgs1*$^{-/-}$ mice. The rapid induction of *Rgs1* following engagement of the antigen receptor in wild-type mice may normally temper premature recruitment of B cells into germinal centers. This may have two functions: (i) to promote the extrafollicular generation of plasma cells and (ii) to limit the number of B cells seeding individual germinal centers. Based on the known elevated expression of *Rgs1* in germinal center B cells and their known refractoriness to chemoattractants, we had expected that *Rgs1* might function to promote the retention of germinal center B cells in developing germinal centers and that the lack of *Rgs1* would lead to short-lived germinal centers in which cells exited prematurely. Without following the kinetics of individual germinal center formation, we cannot fully exclude this scenario; however, the observed *Rgs1*$^{-/-}$ phenotype of excessive and persistent germinal centers did not support this idea. One explanation may be that germinal center B cells not only express *Rgs1*, but they also prominently express *Rgs13* (39). Thus, the lack of *Rgs1* may be compensated for by the presence of *Rgs13*. Studies of *Rgs13*$^{-/-}$ mice and mice lacking both *Rgs1* and *Rgs13* should provide additional insights into germinal B cells trafficking and function.

The loss of the normal sharp delineation between the B- and T-cell zones and misshapen lymphoid follicles, which immunization exaggerated, suggests an interference with the normal directed movement of these cells that occurs during an immune response. This may result, as suggested above, from an inability to properly navigate through a series of chemokine gradients. Both the follicular dendritic cell and stromal cell networks appear intact in the *Rgs1*$^{-/-}$ mice, making the impairment in the production of homing chemokines by *Rgs1*$^{-/-}$ stromal cells an unlikely explanation (CXCL12, CXCL13, and CD11c immunohistochemical staining in the wild-type and *Rgs1*$^{-/-}$ mice appeared similar [C. Moratz, unpublished observation]). Imaging of normal and genetically modified B cells migrating in response to complex chemokine gradients should provide further insights into the role of RGS1 and other RGS proteins in B lymphocyte chemotaxis.

The partial collapse of the Peyer's patches and abnormal trafficking of ASCs in the *Rgs1*$^{-/-}$ mice are likely related. At 1 and 2 weeks following immunization there is a substantial reduction in the size of the Peyer's patches and reduced numbers of ASCs in the spleen, bone marrow, and lamina propria, while the numbers of ASCs in the blood are elevated compared to wild-type mice. Consistent with the spleen ELISPOT data we also observed a reduced number of IgG-positive cells in the bridging channels of the spleen at similar time points, which may account for the lag in the production of IgG noted following immunization. The reduced numbers of ASCs in the spleen of the *Rgs1*$^{-/-}$ mice could be accounted for by either a decreased generation of ASCs or a failure to retain produced cells. Based on the rapid exit of cells from Peyer's patches, the latter seems more likely. The increase of IgG ASCs in the spleen at 1 month may reflect the continued presence of germinal centers in the spleen, which leads to a prolonged generation of ASCs compared to that seen in wild-type mice, where the germinal center response has largely subsided. The heightened number of ASCs in the blood and reduced numbers of ASCs in the bone marrow and lamina propria reflects either the failure of *Rgs1*$^{-/-}$ ASCs to normally enter the bone marrow and lamina propria or, alternatively, a failure of the cells to be normally retained in the end organs. The former seems less likely since *Rgs1*$^{-/-}$ B cells are hyperresponsive to chemokines, while the latter provides a coherent explanation consistent with the known roles of RGS proteins.

CXCL12 promotes the lodgment of IgG-ASCs in the bone marrow (16), while CCL28 promotes the homing of IgA-ASCs to the lamina propria (24). Arguing for the importance of CXCL12 signaling in the localization of IgG-ASCs, CXCR4-deficient ASCs are mislocalized in the spleen, found at increased levels in the blood, and fail to normally accumulate in the bone marrow (16). However, despite their continued CXCR4 expression, IgG-ASCs lose their responsiveness to CXCL12 after lodging in the bone marrow. Between day 6 and day 12 following a secondary immunization with OVA, the percentage of IgG ASCs responsive to CXCL12 in a transwell assay fell from 65% to less than 5% (17). Thus, there is dissociation between CXCR4 expression and CXCL12 responsiveness as is the case with germinal center B cells and with B-cell lines overexpressing RGS1 (33). RGS proteins such as RGS1 may serve as stop signals for migrating cells. While the upregulation of an RGS protein would cause a loss of responsiveness to the localizing chemokine, i.e., the loss of CXCL12 sensitivity of IgG-ASCs, responsiveness to any competing chemoattractants would be lost as well. Whether recent IgA-ASC emigrants into the lamina propria also lose their responsiveness to localizing chemokines is unknown, although the failure of *Rgs1*$^{-/-}$ IgA-ASCs to normally populate the lamina propria following immunization argues that a similar phenomenon occurs.

In conclusion, the development of *Rgs1*$^{-/-}$ mice has revealed an important role for RGS1 in B lymphocytes in the desensitization of signaling through the CXCR4 and CXCR5

receptors, thereby implicating RGS proteins as major regulators of chemokine signaling in B cells and perhaps other immune cell types. The enhanced chemotaxis and exaggerated calcium responses to chemokines observed with unstimulated *Rgs1*$^{-/-}$ B cells indicate that the relatively low level of RGS1 present in nonstimulated normal B cells alters chemokine receptor signaling. Finally, the abnormalities in chemokine signaling likely directly relate to the exaggerated germinal center response and the disruption of architectures of the spleen and Peyer's patches noted following immunization.

ACKNOWLEDGMENTS

We thank C. Pelletier for technical assistance; R. Swafford, C. Eigsti, and D. Stephany of the NIH Flow Cytometry Core Facility for fluorescence-activated cell sorting and Ca^{2+} analysis; M. Rust for her editorial assistance; and Anthony S. Fauci for his continued support.

REFERENCES

1. **Ansel, K. M., and J. G. Cyster.** 2001. Chemokines in lymphopoiesis and lymphoid organ development. Curr. Opin. Immunol. **13:**172–179.
2. **Beadling, C., K. M. Druey, G. Richter, J. H. Kehrl, and K. A. Smith.** 1999. Regulators of G protein signaling exhibit distinct patterns of gene expression and target G protein specificity in human lymphocytes. J. Immunol. **162:** 2677–2682.
3. **Berman, D. M., T. M. Wilkie, and A. G. Gilman.** 1996. GAIP and RGS4 are GTPase-activating proteins for the Gi subfamily of G protein alpha subunits. Cell **86:**445–452.
4. **Bowman, E. P., J. J. Campbell, K. M. Druey, A. Scheschonka, J. H. Kehrl, and E. C. Butcher.** 1998. Regulation of chemotactic and proadhesive responses to chemoattractant receptors by RGS (regulator of G-protein signaling) family members. J. Biol. Chem. **273:**28040–28048.
5. **Campbell, J. J., and E. C. Butcher.** 2000. Chemokines in tissue-specific and microenvironment-specific lymphocyte homing. Curr. Opin. Immunol. **12:** 336–341.
6. **De Vries, L., M. Mousli, A. Wurmser, and M. G. Farquhar.** 1995. GAIP, a protein that specifically interacts with the trimeric G protein G alpha i3, is a member of a protein family with a highly conserved core domain. Proc. Natl. Acad. Sci. USA **92:**11916–11920.
7. **Dietzel, C., and J. Kurjan.** 1987. Pheromonal regulation and sequence of the Saccharomyces cerevisiae SST2 gene: a model for desensitization to pheromone. Mol. Cell. Biol. **7:**4169–4177.
8. **Diverse-Pierluissi, M. A., T. Fischer, J. D. Jordan, M. Schiff, D. F. Ortiz, M. G. Farquhar, and L. De Vries.** 1999. Regulators of G protein signaling proteins as determinants of the rate of desensitization of presynaptic calcium channels. J. Biol. Chem. **274:**14490–14494.
9. **Druey, K. M., K. J. Blumer, V. H. Kang, and J. H. Kehrl.** 1996. Inhibition of G-protein-mediated MAP kinase activation by a new mammalian gene family. Nature **379:**742–746.
10. **El-Sawy, T., N. M. Fahmy, and R. L. Fairchild.** 2002. Chemokines: directing leukocyte infiltration into allografts. Curr. Opin. Immunol. **14:**562–568.
11. **Forster, R., A. E. Mattis, E. Kremmer, E. Wolf, G. Brem, and M. Lipp.** 1996. A putative chemokine receptor, BLR1, directs B cell migration to defined lymphoid organs and specific anatomic compartments of the spleen. Cell **87:**1037–1047.
12. **Forster, R., L. Ohl, and G. Henning.** 2001. Lessons learned from lymphocytes: CC Chemokine receptor-7 involved in lymphogenic metastasis of melanoma. J. Natl. Cancer Inst. **93:**1588–1589.
13. **Foxman, E. F., J. J. Campbell, and E. C. Butcher.** 1997. Multistep navigation and the combinatorial control of leukocyte chemotaxis. J. Cell Biol. **139:** 1349–1360.
14. **Garzon, J., M. Rodriguez-Diaz, A. Lopez-Fando, and P. Sanchez-Blazquez.** 2001. RGS9 proteins facilitate acute tolerance to mu-opioid effects. Eur. J. Neurosci. **13:**801–811.
15. **Gunn, M. D., V. N. Ngo, K. M. Ansel, E. H. Ekland, J. G. Cyster, and L. T. Williams.** 1998. A B-cell-homing chemokine made in lymphoid follicles activates Burkitt's lymphoma receptor-1. Nature **391:**799–803.
16. **Hargreaves, D. C., P. L. Hyman, T. T. Lu, V. N. Ngo, A. Bidgol, G. Suzuki, Y. R. Zou, D. R. Littman, and J. G. Cyster.** 2001. A coordinated change in chemokine responsiveness guides plasma cell movements. J. Exp. Med. **194:**45–56.
17. **Hauser, A. E., G. F. Debes, S. Arce, G. Cassese, A. Hamann, A. Radbruch, and R. A. Manz.** 2002. Chemotactic responsiveness toward ligands for CXCR3 and CXCR4 is regulated on plasma blasts during the time course of a memory immune response. J. Immunol. 160: 1277–1282.
18. **Hepler, J. R., and A. G. Gilman.** 1992. G proteins. Trends Biochem. Sci. **17:**383–387.
19. **Hunt, T. W., T. A. Fields, P. J. Casey, and E. G. Peralta.** 1996. RGS10 is a selective activator of G alpha i GTPase activity. Nature **383:**175–177.
20. **Kehrl, J. H.** 1998. Heterotrimeric G protein signaling: roles in immune function and fine-tuning by RGS proteins. Immunity **8:**1–10.
21. **Koelle, M. R., and H. R. Horvitz.** 1996. EGL-10 regulates G protein signaling in the C. elegans nervous system and shares a conserved domain with many mammalian proteins. Cell **84:**115–125.
22. **Kosco-Vilbois, M. H., J. Y. Bonnefoy, and Y. Chvatchko.** 1997. The physiology of murine germinal center reactions. Immunol. Rev. **156:**127–136.
23. **Kunkel, E. J., and E. C. Butcher.** 2002. Homeostatic chemokines and the targeting of regional immunity. Adv. Exp. Med. Biol. **512:**65–72.
24. **Kunkel, E. J., C. H. Kim, N. H. Lazarus, M. A. Vierra, D. Soler, E. P. Bowman, and E. C. Butcher.** 2003. CCR10 expression is a common feature of circulating and mucosal epithelial tissues IgA Ab-secreting cells. J. Clin. Investig. **111:**1001–1010.
25. **Lee, B. N., and T. H. Adams.** 1994. Overexpression of flbA, an early regulator of Aspergillus asexual sporulation, leads to activation of brlA and premature initiation of development. Mol. Microbiol. **14:**323–334.
26. **Legler, D. F., M. Loetscher, R. S. Roos, I. Clark-Lewis, M. Baggiolini, and B. Moser.** 1998. B cell-attracting chemokine 1, a human CXC chemokine expressed in lymphoid tissues, selectively attracts B lymphocytes via BLR1/CXCR5. J. Exp. Med. **187:**655–660.
27. **Liu, Y. J., and C. Arpin.** 1997. Germinal center development. Immunol. Rev. **156:**111–126.
28. **Lombardi, M. S., A. Kavelaars, and C. J. Heijnen.** 2002. Role and modulation of G protein-coupled receptor signaling in inflammatory processes. Crit. Rev. Immunol. **22:**141–163.
29. **Luster, A. D.** 2002. The role of chemokines in linking innate and adaptive immunity. Curr. Opin. Immunol. **14:**129–135.
30. **MacLennan, I. C., A. Gulbranson-Judge, K. M. Toellner, M. Casamayor-Palleja, E. Chan, D. M. Sze, S. A. Luther, and H. A. Orbea.** 1997. The changing preference of T and B cells for partners as T-dependent antibody responses develop. Immunol. Rev. **156:**53–66.
31. **Manes, S., R. Ana Lacalle, C. Gomez-Mouton, and C. Martinez-A.** 2003. From rafts to crafts: membrane asymmetry in moving cells. Trends Immunol. **24:**320–326.
32. **Melchers, F., A. G. Rolink, and C. Schaniel.** 1999. The role of chemokines in regulating cell migration during humoral immune responses. Cell **12:**351–354.
33. **Moratz, C., V. H. Kang, K. M. Druey, C. S. Shi, A. Scheschonka, P. M. Murphy, T. Kozasa, and J. H. Kehrl.** 2000. Regulator of G protein signaling 1 (RGS1) markedly impairs Gi alpha signaling responses of B lymphocytes. J. Immunol. **164:**1829–1838.
34. **Nagasawa, T., S. Hirota, K. Tachibana, N. Takakura, S. Nishikawa, Y. Kitamura, N. Yoshida, H. Kikutani, and T. Kishimoto.** 1996. Defects of B-cell lymphopoiesis and bone-marrow myelopoiesis in mice lacking the CXC chemokine PBSF/SDF-1. Nature **382:**635–638.
35. **Neer, E. J.** 1995. Heterotrimeric G proteins: organizers of transmembrane signals. Cell **80:**249–257.
36. **Potenza, M. N., S. J. Gold, A. Roby-Shemkowitz, M. R. Lerner, and E. J. Nestler.** 1999. Effects of regulators of G protein-signaling proteins on the functional response of the mu-opioid receptor in a melanophore-based assay. J. Pharmacol. Exp. Ther. **291:**482–491.
37. **Proudfoot, A. E.** 2002. Chemokine receptors: multifaceted therapeutic targets. Nat. Rev. Immunol. **2:**106–115.
38. **Reif, K., and J. G. Cyster.** 2000. RGS molecule expression in murine B lymphocytes and ability to down-regulate chemotaxis to lymphoid chemokines. J. Immunol. **164:**4720–4729.
39. **Shi, G.-X., K. Harrison, G. L. Wilson, C. Moratz, and J. H. Kehrl.** 2002. RGS13 regulates germinal center B-lymphocytes responsiveness to CXCL12 and CXCL13. J. Immunol. **169:**2507–2515.
40. **Sierra, D. A., D. J. Gilbert, D. Householder, N. V. Grishin, K. Yu, P. Ukidwe, S. A. Barker, W. He, T. G. Wensel, G. Otero, G. Brown, N. G. Copeland, N. A. Jenkins, and T. M. Wilkie.** 2002. Evolution of the regulators of G-protein signaling multigene family in mouse and human. Genomics **79:**177–185.
41. **Srinivasa, S. P., L. S. Bernstein, K. J. Blumer, and M. E. Linder.** 1998. Plasma membrane localization is required for RGS4 function in Saccharomyces cerevisiae. Proc. Natl. Acad. Sci. USA **95:**5584–5589.
42. **Tarlinton, D.** 1998. Germinal centers: form and function. Curr. Opin. Immunol. **10:**245–251.
43. **Wang, Q., M. Liu, B. Mullah, D. P. Siderovski, and R. R. Neubig.** 2002. Receptor-selective effects of endogenous RGS3 and RGS5 to regulate mitogen-activated protein kinase activation in rat vascular smooth muscle cells. J. Biol. Chem. **277:**24949–24958.
44. **Watson, N., M. E. Linder, K. M. Druey, J. H. Kehrl, and K. J. Blumer.** 1996. RGS family members: GTPase-activating proteins for heterotrimeric G-protein alpha-subunits. Nature **383:**172–175.
45. **Wehrli, N., D. F. Legler, D. Finke, K. M. Toellner, P. Loetscher, M. Baggiolini, I. C. MacLennan, and H. Acha-Orbea.** 2001. Changing responsiveness to chemokines allows medullary plasmablasts to leave lymph nodes. Eur. J. Immunol. **31:**609–616.
46. **Zou, Y. R., A. H. Kottmann, M. Kuroda, I. Taniuchi, and D. R. Littman.** 1998. Function of the chemokine receptor CXCR4 in haematopoiesis and in cerebellar development. Nature **393:**595–599.